

Article

Lithogenic and Anthropogenic Components in Surface Sediments from Lake Limboto as Shown by Magnetic Mineral Characteristics, Trace Metals, and REE Geochemistry

Raghel Yunginger ^{1,*} , Satria Bijaksana ¹ , Darharta Dahrin ¹, Siti Zulaikah ², Abd Hafidz ¹ , Kartika Hajar Kirana ³, Sudarningsih Sudarningsih ⁴ , Mariyanto Mariyanto ⁵  and Silvia Jannatul Fajar ¹ 

¹ Faculty of Mining and Petroleum Engineering, Institut Teknologi Bandung, Jalan Ganesha 10, Bandung 40132, Indonesia; satria@fi.itb.ac.id (S.B.); dahrin@gf.itb.ac.id (D.D.); abdulhafidz6@gmail.com (A.H.); silviajannatulfajar@gmail.com (S.J.F.)

² Faculty of Mathematics and Natural Sciences, Universitas Negeri Malang, Malang 65145, Indonesia; siti.zulaikah.fmipa@um.ac.id

³ Faculty of Mathematics and Natural Sciences, Universitas Padjadjaran, Jatinangor 45363, Indonesia; kartika@geophys.unpad.ac.id

⁴ Faculty of Mathematics and Natural Sciences, Universitas Lambung Mangkurat, Banjarmasin 70124, Indonesia; sudarningsih01@unlam.ac.id

⁵ Faculty of Civil, Environmental and Geo Engineering, Institut Teknologi Sepuluh Nopember, Surabaya 60111, Indonesia; mariyanto@geofisika.its.ac.id

* Correspondence: raghel@ung.ac.id; Tel.: +62-852-206-26075

Received: 24 February 2018; Accepted: 27 March 2018; Published: 31 March 2018



Abstract: Lake Limboto is one of the major lakes in Sulawesi, Indonesia. It is currently undergoing serious degradation due to population pressure. As more residential areas have been established around the lake, the sedimentation rate has increased because of the contribution of anthropogenic particles. In this study, the lithogenic and anthropogenic components in surface sediments from 17 points in the lake were studied and identified using a combination of magnetic and geochemical analyses. The results showed that although the magnetic susceptibility values in R (residential) and NR (non-residential) areas were relatively similar, the values of saturation isothermal remanent magnetization (SIRM) as well as those of $SIRM/\chi_{LF}$ differed significantly, implying that the magnetic characteristics of the lithogenic component (in the NR area) differ from those of the anthropogenic component (in the R area). The discrepancy between the anthropogenic and lithogenic contributions was further supported by trace metals and rare earth element (REE) contents. Sediment samples in the R area contained higher levels of Mn, La, Pr, and Gd, while in the NR area they contained higher levels of Fe, Sc, Nd, and Ce. The magnetic susceptibility also correlated strongly with Fe, Cu, Zn, and Mn contents in the NR area. A similar correlation was not observed in the R area. The results above imply that a combination of magnetic and geochemical analyses can successfully differentiate lithogenic and anthropogenic components or contributions in lake sediments.

Keywords: lithogenic; anthropogenic; Lake Limboto; magnetic minerals; trace metals; rare earth elements; surface sediment

1. Introduction

Lake Limboto in the Gorontalo Province, Sulawesi, is one of several lakes in Indonesia that faces serious degradation due to population pressure as more residential areas are established in the vicinity

of the lake. As the sedimentation rate has increased, the lake has reduced to about 3000 hectares in size with a depth of only 2–4 m [1]. The sources of sediment entering into the lake are no longer natural in origin but are also anthropogenic. Like many other lakes, sedimentation in a lacustrine environment (as in Lake Limboto) is formed as a closed system with a relatively high deposition rate when compared to that of a marine environment. Generally, lacustrine sediments contain magnetic minerals and trace metals originating from lithogenic sources, from in situ processes in the lakes, as well as from anthropogenic sources [2–4]. The term “trace metals” has been used in earlier studies to describe lithogenic as well as anthropogenic metals [5,6]. In this study, lithogenic components are defined as those components produced from the weathering of bedrocks and soils in the catchment area that were transported either by water or by air, which then settled at the lake bottom. Thus, the magnetic minerals or trace metals in the lake sediments were related to those in the bedrocks and soils. For instance, the lake sediments from areas with basalt and ultramafic bedrocks had a higher magnetic susceptibility (a higher concentration of magnetic minerals) when compared to lake sediments from areas with limestone bedrocks [7,8].

More recent studies have shown that the variations in the content of magnetic minerals in lake sediments are controlled not only by lithogenic components but also by coarse-grained magnetite anthropogenic provenience. Anthropogenic contributions can also be identified by an increase in trace metal content. For instance, studies of sediments from Lake Champlain [9], East Lake [10], and Lake Sanliqi [11] have reported an increase in magnetic susceptibility followed by an increase in the trace metals Fe, Mn, Cu, Zn, Cr, Pb, and Cd from several forms of anthropogenic waste. Additionally, coarse grain magnetite (Fe_3O_4) with PSD (pseudo-single domain)/MD (multi-domain) sizes were found in East Lake [10,12] and Lake Gonghai [13] that were contaminated not only from mining, industrial, agricultural, and residential wastes but also from vehicle emissions. Moreover, magnetic minerals with similar properties have also been found in river sediments [14–17], soil [18–20], and leachate [21–23] that were anthropogenic.

In this study, lithogenic and anthropogenic components in surface sediments from Lake Limboto were identified based on their magnetic and geochemical characteristics. On the basis of these characteristics, it was possible to map the areas of the lake affected by lithogenic and/or anthropogenic components. The results of this study are expected to become a baseline for monitoring and assessing lithogenic and anthropogenic contributions in lakes, especially Lake Limboto.

2. Materials and Methods

Lake Limboto is a tectonic lake located in the northern part of Sulawesi Island, Gorontalo, Indonesia. Geologically, Lake Limboto is part of the Gorontalo depression that allegedly lifted as a result of the influence of the Sangihe subduction in the Plio-Pleistocene. This is demonstrated by the coral growth that formed limestone rocks with a high elevation [24–26]. This process of geological dynamics formed the bedrock of Lake Limboto, which is dominated by limestone rocks, coral being the main component. The main residential areas around the lake are mostly located on the eastern and northern coasts (Figure 1). There are 23 rivers to the north, west, and south of the lake that serve as inlets for Lake Limboto. The main rivers are the Alopohu, Bionga, Talubongo, Moluopo, Marisa, and Rintenga Rivers. However, Lake Limboto has only one outlet, the Tapodu River in the south-eastern part of the lake, which flows towards Gorontalo Bay.

Samples of surface sediments were collected from 17 points in Lake Limboto (Figure 1) using a sediment grabber. On the basis of the proximity from the residential areas on the coast, the samples were divided into two groups: R (for residential) and NR (for non-residential) zones. In the R zones, the immediate coast has dense residential areas. In the NR zones, the coast is sparsely populated. Some areas of the lake, especially in the western part, are used extensively for fish farming. The presence of fishnets prohibited symmetrical sampling. In total, eleven sampling points (1 to 9, 12, 13) were designated as R points while the other six sampling points (10, 11, 14 to 17) were designated as NR points.

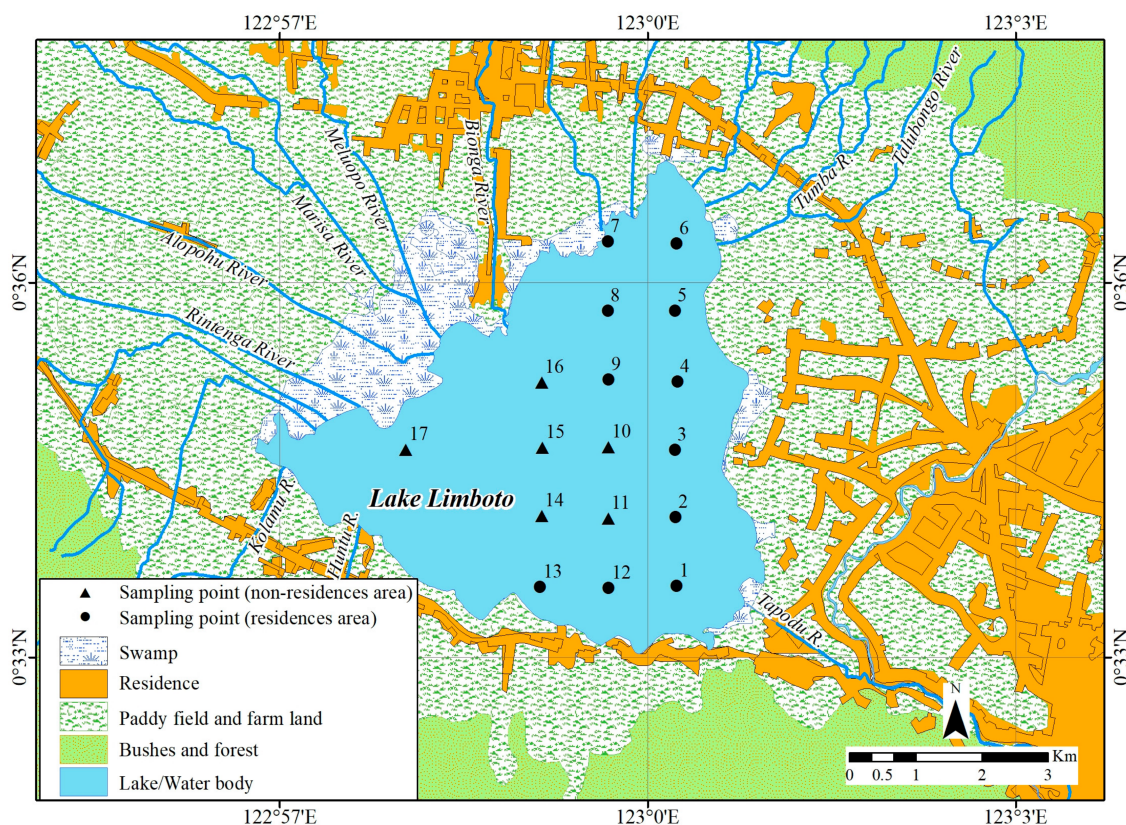


Figure 1. Map of Lake Limboto and the 17 sample points used for the collection of surface sediments. Sampling Points 1 to 9, 12, 13 are in the residential (R) area (●) and sampling points 10, 11, 14 to 17 are in the non-residential (NR) area (▲).

Sediment samples were then sieved with a 325-mesh sized (44 μm in diameter) sieve to obtain homogeneous clay particles. These were prepared for magnetism measurements as well as measurements of trace metals and rare earth element (REE) contents. Detailed sample preparations and measurements for magnetic parameters were carried out following the steps described earlier in Reference [27]. In this study, the measured and determined magnetic parameters included mass-based low-frequency magnetic susceptibility (χ_{LF}), frequency-dependent magnetic susceptibility ($\chi_{\text{FD}} \%$), and isothermal remanent magnetization (IRM), as well as saturation isothermal remanent magnetization (SIRM). All of these measurements were conducted in the laboratories at the Institut Teknologi Bandung, Indonesia.

The χ_{LF} (in m^3/kg) was used to infer the concentrations of magnetic minerals controlled mainly by ferromagnetic (*sensu lato*) mineral phases such as magnetite and hematite [2,3,27,28]. The $\chi_{\text{FD}} \%$ analysis was used to determine the portion of superparamagnetic (SP) fine grains in the samples. Low values of $\chi_{\text{FD}} \%$ (<2%) infers that there were no SP grains in the sample, while very high values of $\chi_{\text{FD}} \%$ (>14%) infers that the sample only contained SP grains. When the $\chi_{\text{FD}} \%$ value is between 2–14%, the sample contained a mixture of SP and non-SP grains [28,29]. In addition, the IRM parameter was also analyzed to identify the magnetic mineral phases with low and high coercivity. Moreover, the SIRM parameter ($10^{-6} \text{ A}\cdot\text{m}^2/\text{kg}$) was used to indicate the magnetic mineral concentration total of the ferrimagnetic phases with greater grain sizes than SP or single domain (SD) [2,21].

Trace metal concentrations were determined by atomic absorption spectroscopy (AAS) analyses using an AA280FS (Varian Inc., Palo Alto, CA, USA) instrument at the laboratory of the Indonesian Geological Survey in Bandung, Indonesia. REE concentrations were measured by Inductively Coupled Plasma Atomic-Optical Emission Spectrometry (ICP-OES) analysis using the Agilent type 700/725 ICP-OES instrument (Agilent Technologies, Santa Clara, CA, USA) at the Laboratory of the Center

for Mineral and Coal Resources in Bandung, Indonesia. The reference material was Bushveld granite from Transvaal, South Africa, certified by the Council for Mineral Technology (MINTEK) P/Bag X3015, Randburg 2125, Republic of South Africa. In this study, all REEs are from La through Lu + Y. However, as the measurements were carried out using the ICP-OES method, the REE concentrations were normalized to the North American Shale Composite (NASC) [30].

3. Results and Discussion

3.1. Results

Results of the magnetic measurements and analyses are summarized in Table 1. It shows that χ_{LF} varied from point to point, but the mean values for the R and NR areas were rather different ($55.02 \times 10^{-8} \text{ m}^3/\text{kg}$ for the R area and $62.67 \times 10^{-8} \text{ m}^3/\text{kg}$ for the NR area). Figure 2 shows that the IRM curves for representative samples from the R area (represented by the sample from point 2) and from the NR area (represented by the sample from point 17) were saturated in the applied field of less than 300 mT. This implies that the magnetic minerals contained in these two representative samples were predominated by ferromagnetic minerals with low coercivity, such as magnetite (Fe_3O_4). Assuming that magnetite is the predominant magnetic mineral in these samples, the abundance of magnetite (in %) can then be estimated by dividing the SIRM value by the magnetization saturation for magnetite (J_{sm}) ($9.2 \text{ Am}^2/\text{kg}$) [2]. The results showed that the mean value of % magnetite in the R area (0.16‰) was slightly higher than in the NR area (0.11‰) (Table 1). Moreover, dissimilarities between the R and NR samples were also observed in the values of SIRM and SIRM/χ_{LF} . The mean SIRM value for the R samples was $146.48 \times 10^{-6} \text{ Am}^2/\text{kg}$ when compared to $99.82 \times 10^{-6} \text{ Am}^2/\text{kg}$ for the NR samples. The mean SIRM/χ_{LF} value for the R samples was 263.87 A/m when compared to 156.80 A/m for the NR samples. These differences imply that the anthropogenic and lithogenic contributions to lake sediments could be identified by magnetic parameters, i.e., % magnetite, SIRM, and SIRM/χ_{LF} . Such differences can be observed in Figure 3 where the χ_{LF} distribution (see Figure 3a) differs from the distributions of SIRM and % magnetite (see Figure 3b,c).

Table 1. Magnetic parameters of selected surface sediments in the R and NR areas of Lake Limboto. SIRM: saturation isothermal remanent magnetization.

Zones	Sampling Points	χ_{LF} ($10^{-8} \text{ m}^3/\text{kg}$)	χ_{FD} %	SIRM ($10^{-6} \text{ Am}^2/\text{kg}$)	% Magnetite (‰)	SIRM/χ_{LF} (Am^{-1})
R area	1	64.92	5.39	181.87	0.20	280.24
	2	64.10	2.65	216.86	0.24	338.31
	3	57.94	3.80	182.98	0.20	316.03
	4	50.82	4.74	204.98	0.22	403.50
	5	45.84	5.46	109.10	0.12	238.21
	6	53.88	3.15	108.70	0.12	201.68
	7	72.00	4.03	166.48	0.18	231.23
	8	57.30	4.89	133.24	0.14	232.53
	9	48.82	5.12	122.00	0.13	250.01
	12	44.16	5.20	64.19	0.07	145.22
	13	45.54	1.76	120.85	0.13	265.61
	Max	72.00	5.46	216.86	0.24	403.50
	Min	44.16	1.76	64.19	0.07	145.22
Mean	55.02	4.20	146.48	0.16	263.87	
NR area	10	55.28	6.30	84.98	0.09	153.67
	11	52.42	5.73	74.51	0.08	142.19
	14	51.00	5.88	67.27	0.07	131.91
	15	67.40	4.75	116.55	0.13	172.92
	16	68.00	4.26	112.36	0.12	165.23
	17	81.94	3.79	143.23	0.16	174.89
	Max	81.94	6.30	143.23	0.16	174.89
	Min	51.00	3.79	67.27	0.07	131.91
Mean	62.67	5.12	99.82	0.11	156.80	

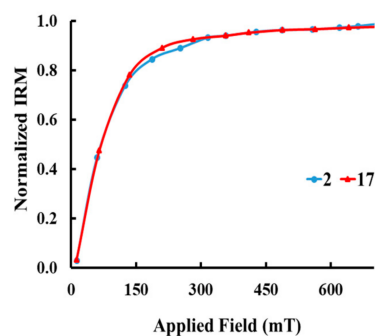


Figure 2. Isothermal remanent magnetization (IRM) curves saturated below 300 mT in the R area (represented by point 2) and the NR area (represented by point 17) indicates a ferromagnetic mineral phase such as magnetite (Fe_3O_4).

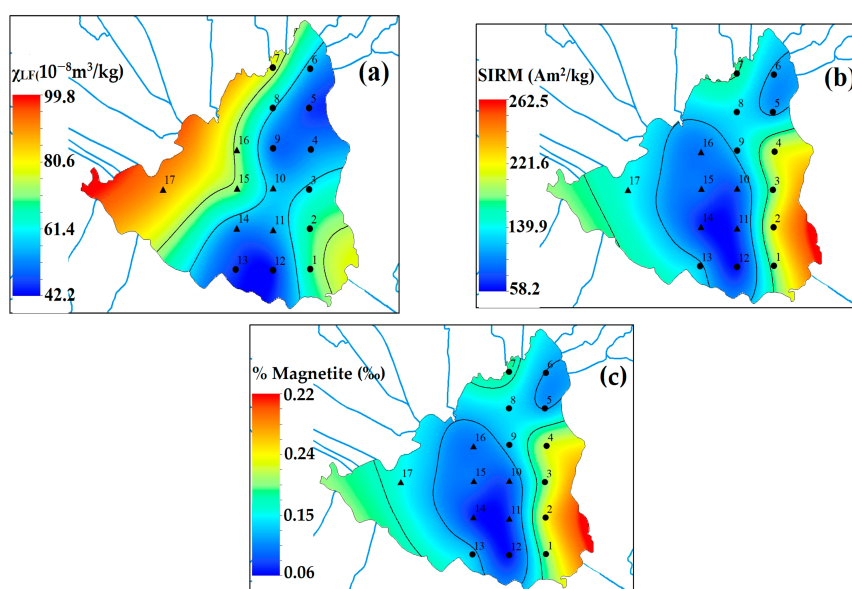


Figure 3. The distribution patterns of magnetic parameters; (a) magnetic minerals abundance (χ_{LF}); (b) saturation isothermal remanent magnetization (SIRM); (c) % magnetite abundance in the R and NR areas.

Table 2 shows the results of the geochemical analyses. The trace metal (Fe, Mn, Zn, Cu, and Ni) contents for the sediment samples from the R area differed from those from the NR area. The NR area was marked by a high Fe content (mean of 100.53 ppm) while the R area was marked by a high Mn content (mean of 5.21 ppm). Meanwhile, the mean values of the Zn, Cu, and Ni contents were rather similar for both the R and NR areas. Figure 4 shows the distribution of Fe and Mn values in the sediments. Table 2 included only seven REEs which were identified using ICP-OES (La, Ce, Pr, Nd, Gd, Sc, and Y). Apparently, the REE (La, Ce, Pr, Nd, Gd, and Sc) concentrations in the R and NR areas were also different. The samples in the R area had higher mean values of La, Pr, and Gd, while the samples from the NR area had higher mean values of Ce, Nd, and Sc. Differences in the REE concentration could also be observed in Figure 5. In the R area, concentrations of La, Pr, and Gd were higher, especially in points 1–3, and in points 7–9 (Figure 5a–c). Meanwhile, the NR area was characterized by a predominance of Ce, Nd, and Sc, which tended to be higher at points 14–17 (Figure 5e–g). These results showed that anthropogenic and lithogenic contributions to lake sediments could also be identified by trace metals and REE contents. Anthropogenic contributions were marked by high contents of Mn, La, Pr, and Gd, while the lithogenic contributions were marked by high contents of Fe, Ce, Nd, and Sc. Table 2 also shows that the areas of R and NR are distinguished by the

mean value of the ratio $(La/Gd)_{NASC}$. The NR area is marked by a mean $(La/Gd)_{NASC}$ value of 0.78, higher than the R area (0.24). This implies that the concentrations of light REE (La, Ce, Pr, Nd) are higher in bedrock than heavy REE (Gd) [31]. The results of this study indicate that the high value of $(La/Gd)_{NASC}$ becomes a characteristic marker of lithogenic components, especially for the conditions found in Lake Limboto.

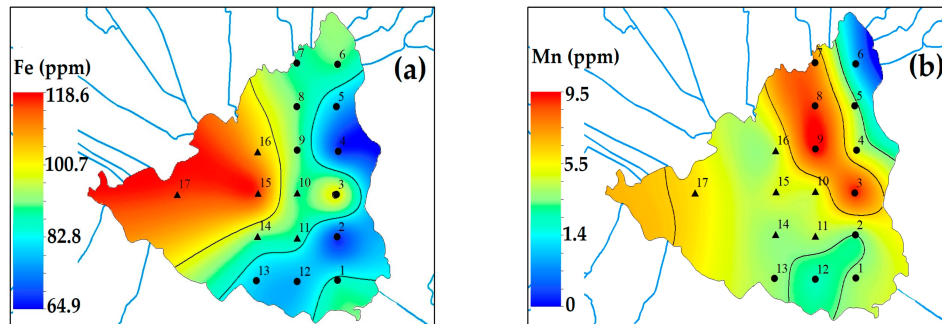


Figure 4. The distribution patterns of trace metal contents: (a) Fe metal has a high concentration in the NR area, mainly at points 14–17 (orange areas); (b) Mn metal has a high concentration in the R area mainly at points 3, 7, 8 and 9 (orange areas).

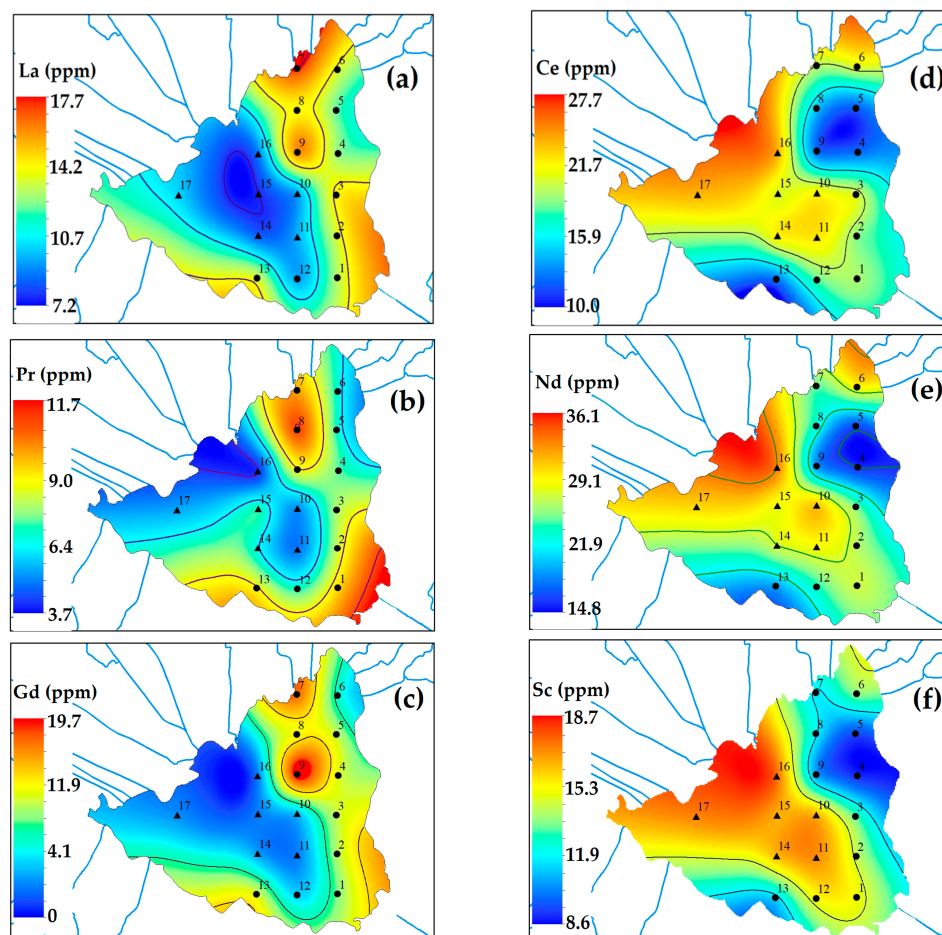


Figure 5. The different distribution patterns of the rare earth element (REE) contents in the R and NR areas. The R area is characterized by a high concentration of La, Pr, and Gd (a–c); and the NR area is characterized by a high concentration of Ce, Nd, and Sc (d–f).

Table 2. Concentrations of selected trace metals, REE, North American Shale Composite (NASC)-normalized REE contents, as well as (Gd/La)_{NASC} ratios in surface sediments of R and NR areas.

Zones	Sampling Points	Trace Metal Concentrations (ppm)					REE Concentrations (ppm)							(REEs) _{NASC}					(La/Gd) _{NASC}		
		Fe	Mn	Zn	Cu	Ni	La	Ce	Pr	Nd	Sc	Gd	Y	La	Ce	Pr	Nd	Sc		Gd	
R area	1	85.71	3.84	0.33	0.18	-	12.76	18.32	9.17	26.92	15.09	8.05	8.84	0.41	0.27	1.83	0.98	1.01	1.61	0.25	
	2	68.19	3.35	0.27	0.12	-	13.24	17.85	8.09	26.34	14.41	9.27	8.78	0.43	0.27	1.62	0.96	0.97	1.85	0.23	
	3	100.10	9.04	0.60	0.26	0.03	13.96	19.40	7.81	24.98	13.23	9.89	9.58	0.45	0.29	1.56	0.91	0.89	1.98	0.23	
	4	68.42	4.79	0.51	0.14	-	12.39	12.17	7.31	15.87	9.06	10.74	7.14	0.40	0.18	1.46	0.58	0.61	2.15	0.19	
	5	77.83	3.83	0.41	0.17	0.02	11.93	11.77	6.92	16.60	9.44	9.82	7.05	0.38	0.18	1.38	0.61	0.63	1.96	0.20	
	6	90.00	0.35	0.83	0.33	-	13.39	19.47	6.76	28.67	13.61	5.61	9.14	0.43	0.29	1.35	1.05	0.91	1.12	0.38	
	7	88.13	7.59	0.44	0.21	0.06	16.67	18.73	9.77	24.47	11.77	17.08	11.84	0.54	0.28	1.95	0.89	0.79	3.42	0.16	
	8	90.93	8.74	0.41	0.20	0.03	13.94	14.09	10.75	22.73	11.97	11.62	9.02	0.45	0.21	2.15	0.83	0.80	2.32	0.19	
	9	91.44	9.40	0.40	0.16	-	15.54	12.26	8.49	18.88	10.75	19.36	7.89	0.50	0.18	1.70	0.69	0.72	3.87	0.13	
	12	77.02	2.56	0.46	0.17	-	9.42	17.23	7.03	23.63	15.18	2.82	7.01	0.30	0.26	1.41	0.86	1.02	0.56	0.54	
	13	79.46	3.85	0.30	0.10	-	13.22	12.35	8.71	19.26	11.53	10.66	6.43	0.43	0.19	1.74	0.70	0.77	2.13	0.20	
		Max	100.10	9.40	0.83	0.33	0.06	16.67	19.47	10.75	28.67	15.18	19.36	11.84	0.54	0.29	2.15	1.05	1.02	3.87	0.54
		Min	68.19	0.35	0.27	0.10	0.02	9.42	11.77	6.76	15.87	9.06	2.82	6.43	0.30	0.18	1.35	0.58	0.61	0.56	0.13
	Mean	83.38	5.21	0.45	0.19	0.04	13.31	15.79	8.26	22.58	12.37	10.45	8.43	0.43	0.24	1.65	0.82	0.83	2.09	0.24	
NR area	10	89.32	4.84	0.45	0.14	0.02	9.45	20.49	5.26	30.49	16.45	2.33	8.33	0.30	0.31	1.05	1.11	1.10	0.47	0.65	
	11	87.09	4.19	0.43	0.16	-	9.52	20.96	4.98	28.39	16.99	0.00	8.14	0.31	0.31	1.00	1.04	1.14	0.00	-	
	14	90.76	3.67	0.35	0.13	0.05	8.37	20.68	6.51	27.18	16.36	1.14	7.08	0.27	0.31	1.30	0.99	1.10	0.23	1.18	
	15	115.00	4.77	0.65	0.17	0.08	7.71	19.60	7.04	28.25	16.57	0.00	7.27	0.25	0.29	1.41	1.03	1.11	0.00	-	
	16	106.00	4.36	0.52	0.20	0.03	8.81	22.22	4.29	32.70	17.53	0.00	8.53	0.28	0.33	0.86	1.19	1.18	0.00	-	
	17	115.00	5.98	0.50	0.22	0.08	10.05	22.18	5.49	30.00	17.16	0.57	9.35	0.32	0.33	1.10	1.09	1.15	0.11	2.83	
		Max	115.00	5.98	0.65	0.22	0.08	10.05	22.22	7.04	32.70	17.53	2.33	9.35	0.32	0.33	1.41	1.19	1.18	0.47	2.83
		Min	87.09	3.67	0.35	0.13	0.02	7.71	19.60	4.29	27.18	16.36	0.00	7.08	0.25	0.29	0.86	0.99	1.10	0.00	0.65
	Mean	100.53	4.64	0.48	0.17	0.05	8.99	21.02	5.60	29.50	16.84	0.67	8.12	0.29	0.32	1.12	1.08	1.13	0.13	0.78	

3.2. Discussion

The magnetic properties of the minerals in the surface sediments of Lake Limboto had a lower magnetic mineral abundance than those derived from Lake Towuti and Lake Matano [8,32]. Although Lake Towuti and Lake Matano are on Sulawesi Island, the bedrocks are ultramafic, which is very different from the limestone in the vicinity of Lake Limboto. The magnetic mineral content in basalt is much higher than that in limestone [2,7,8,32]. Therefore, it is not surprising that the χ_{LF} values in Lake Limboto tended to be lower than those found in the other lakes.

Compared to those from the NR area, samples from the R area had similar mean χ_{LF} values, but higher mean SIRM and SIRM/ χ_{LF} values. This implies that the relative quantity of magnetic minerals in the R area was higher than in the NR area (also shown by a higher % magnetite). The SIRM and % magnetite distributions (Figure 3b,c) were very similar. Higher SIRM values for polluted areas (resulting from vehicle emissions, residential and industrial wastes) have also been reported in previous studies [20,33,34]. The similarity in the mean χ_{FD} % values for samples in the R and NR areas (Table 1) implies that the samples contained both SP and non-SP grains [2,28,29]. However, the SIRM/ χ_{LF} values differed significantly. Earlier studies showed that polluted sediments exhibit high SIRM/ χ_{LF} [22,27]. Another earlier study also showed that polluted sediments contained PSD and MD magnetite grains [20,35–37]. Our findings—that magnetic parameters can be used to identify lithogenic and anthropogenic components in lake sediments—are supported by these assertions.

Table 3 shows the correlations between the χ_{LF} , trace metals, and REE contents. Interestingly, in the NR area, χ_{LF} correlated well with Fe ($r = 0.91$, $p = 0.05$) as well as with other trace metals. In contrast, in the R area, there was no correlation between the χ_{LF} and trace metal content. However, in the R area, χ_{LF} correlated well with Ce and Nd. These results imply that in the NR area, the sources of magnetic minerals were the same as the sources of trace metals, i.e., particulates of lithogenic origin. Similar findings have been previously reported [12,19].

Table 3. Pearson correlation coefficients (r) at $p = 0.05$ between χ_{LF} and trace metal contents as well as REE contents in the samples in the R area ($n = 11$) and NR area ($n = 6$). The bold marker indicates a significant correlation between two parameters.

	Parameters	Fe	Cu	Zn	Mn	La	Ce	Pr	Nd	Sc	Gd
R area	χ_{LF}	0.21	0.22	−0.09	0.24	0.58	0.64	0.54	0.60	0.33	0.27
	Fe		0.67	0.42	0.54	0.51	0.35	0.33	0.35	0.14	0.28
	Cu			0.88	−0.05	0.19	0.62	−0.16	0.57	0.25	−0.20
	Zn				−0.20	0.01	0.39	−0.46	0.29	0.03	−0.28
	Mn					0.63	−0.18	0.60	−0.24	−0.33	0.75
	La						0.10	0.57	0.10	−0.27	0.85
	Ce							0.08	0.93	0.84	−0.37
	Pr								0.13	0.31	0.52
	Nd									0.87	−0.37
	Sc										−0.56
NR area	χ_{LF}	0.91	0.92	0.65	0.84	0.23	0.50	−0.07	0.44	0.56	−0.35
	Fe		0.77	0.80	0.65	−0.19	0.19	0.23	0.26	0.39	−0.48
	Cu			0.50	0.71	0.36	0.70	−0.37	0.57	0.83	−0.54
	Zn				0.46	−0.38	−0.21	0.22	0.25	0.24	−0.54
	Mn					0.52	0.32	−0.07	0.33	0.29	0.04
	La						0.63	−0.64	0.34	0.39	0.25
	Ce							−0.74	0.65	0.83	−0.20
	Pr								−0.78	−0.74	0.04
	Nd									0.72	−0.01
	Sc										−0.60

In the R area, the sources of magnetic minerals sometimes differed from those of trace metals, implying a complexity of anthropogenic sources [19,38]. The abundance of Mn as an indication of anthropogenic contributions (industrial and mining activities) to sediments has also been reported in Lake Sanliqi [11]. A high Mn content has also been reported as originating from agricultural waste, residential waste [39], electronic waste, fossil fuel emissions [40], industrial waste, and traffic

emissions [41]. The REE in the aquatic environment might come from the weathering of rocks and also from pollutants caused by human activities [42–45]. High REE contents have been reported in the sediment of Lake Dojran caused by agricultural fertilizers [46]. Previous studies have reported that La and Gd were found in urban and hospital waste [31,47,48]. Gd has found wide applications in magnetic resonance imaging (MRI) as a contrasting reagent. The stable Gd chelates may be released with antibiotics, antihypertensive, anti-inflammatories, antihistamines, and estrogens from medical facilities into municipal sewage systems and then into streams and rivers [31,48]. This supports our findings that high levels of La, Gd, and Pr are anthropogenic rather than lithogenic.

4. Conclusions

The magnetic mineral properties in the R and NR areas were differentiated by their SIRM and SIRM/ χ_{LF} values. The R area was characterized by coarse-grained (PSD- and MD-sized) magnetite, indicating an anthropogenic contribution. In contrast, the NR area was characterized by finer (PSD-sized) magnetite, indicating a lithogenic contribution. The R area was also characterized by higher concentrations of Mn, La, Pr, and Gd while the NR area was characterized by higher concentrations of Fe, Ce, Nd, and Sc. In the NR area, the magnetic susceptibility strongly correlated with the trace content, implying that the magnetic minerals originated from the same sources as those of the trace metals. Such a correlation was not found in the R area, implying that the anthropogenic components might have originated from various sources including residential, agricultural, and industrial wastes. We propose that in an environmental setting like that of Lake Limboto, higher SIRM and SIRM/ χ_{LF} values in surface sediments indicate predominantly anthropogenic contributions, while low values of SIRM and SIRM/ χ_{LF} indicate lithogenic contributions.

Acknowledgments: This research was financially funded by the Ministry of Research, Technology, and Higher Education of the Republic of Indonesia to Satria Bijaksana. Additional fundings were received in the forms of doctoral fellowship and doctoral research grant to Raghel Yunginger also from the Ministry. Sediments from Lake Limboto were collected with permission from Gorontalo Province. Abd Mujahid Hamdan, Nono Agus Santoso, and Aditya Pratama are thanked for their assistance in the field and during the laboratory work. We thank two anonymous reviewers for their constructive comments.

Author Contributions: Raghel Yunginger, Satria Bijaksana, Darharta Dahrin and Siti Zulaikah conceived the idea for this study. Raghel Yunginger, Satria Bijaksana, Abd Hafidz and Mariyanto Mariyanto collected the samples. Raghel Yunginger, Satria Bijaksana, Sudarningsih Sudarningsih, Silvia Jannatul Fajar and Kartika Hajar Kirana measured the samples. Raghel Yunginger, Satria Bijaksana, Darharta Dahrin, Siti Zulaikah, Abd Hafidz, Sudarningsih Sudarningsih, Kartika Hajar Kirana and Silvia Jannatul Fajar prepared the manuscript.

Conflicts of Interest: The authors declare no conflicts of interest.

References

1. Putra, S.S.; Hasan, C.; Djudi; Suryatmojo, H. Reservoir saboworks solutions in Limboto Lake sedimentations, Northern Sulawesi, Indonesia. *J. Procedia Environ. Sci.* **2013**, *17*, 230–239. [[CrossRef](#)]
2. Evans, M.E.; Heller, F. *Environmental Magnetism: Principles and Application of Environmagnetics*; Academic Press: Burlington, MA, USA, 2003; pp. 9–164. ISBN 0122438515.
3. Dunlop, D.J.; Özdemir, Ö. *Rock Magnetism Fundamental and Frontiers*; Cambridge University Press: Cambridge, UK, 1997; pp. 5–445. ISBN 052100098X.
4. Williamson, D.; Jelinowska, A.; Kissel, C.; Tucholka, P.; Gibert, E.; Gsese, F.; Massault, M.; Taib, M.; Van Compo, E.; Wieckowski, K. Mineral magnetic proxies of erosion/oxidation cycles in topical maar lake sediments (Lake Tritrivakely, Madagascar); paleoenvironmental Implication. *Earth Planet. Sci. Lett.* **1998**, *155*, 205–219. [[CrossRef](#)]
5. Kabata-Pendias, A. Behavioural properties of trace metals in soils. *Appl. Geochem.* **1993**, *8*, 3–9. [[CrossRef](#)]
6. Kabata-Pendias, A.; Mukherjee, A.B. *Trace Elements from Soil to Human*; Springer: Berlin, Germany, 2007; pp. 1–2. ISBN 3540327134.
7. Hunt, C.P.; Moskowitz, B.M.; Banerjee, S.K. Magnetic properties of rock and minerals. In *Rock Physics and Phase Relation—A Handbook of Physical Constant*; Ahrens, T.J., Ed.; American Geophysical Union: Washington, DC, USA, 1995; pp. 189–204. ISBN 0875908535.

8. Tamuntuan, G.; Bijaksana, S.; King, J.; Russell, J.; Fauzi, U.; Maryunani, K.; Aufa, N.; Safiuddin, L.O. Variation of magnetic properties in sediments from Lake Towuti, Indonesia, and its paleoclimate significance. *Palaeogeogr. Palaeoclimatol. Palaeoecol.* **2015**, *420*, 163–172. [[CrossRef](#)]
9. Mecray, E.L.; King, J.W.; Appleby, P.G.; Hunt, A.S. Historical trace metal accumulation in the sediments of an urbanized region of the Lake Champlain watershed, Burlington, Vermont. *Water Air Soil Pollut.* **2001**, *125*, 201–230. [[CrossRef](#)]
10. Yang, T.; Liu, Q.; Chan, L.; Liu, Z. Magnetic signature of heavy metals pollution of sediments: Case study from the East Lake in Wuhan, China. *Environ. Geol.* **2007**, *52*, 1639–1650. [[CrossRef](#)]
11. Zeng, L.; Ning, D.; Xu, L.; Mao, X.; Chen, X. Sedimentary evidence of environmental degradation in Sanliqi Lake, Daye City (A Typical Mining City, Central China). *Bull. Environ. Contam. Toxicol.* **2015**, *95*, 317–324. [[CrossRef](#)] [[PubMed](#)]
12. Yang, T.; Liu, Q.; Zeng, Q.; Chan, L. Environmental magnetic responses of urbanization processes: Evidence from lake sediments in East Lake, Wuhan, China. *Geophys. J. Int.* **2009**, *179*, 873–886. [[CrossRef](#)]
13. Bao, L.J.; Hu, C.F.; Hui, C.J.; Sheng, X.D.; Hai, X.Q. Humid Medieval warm period recorded by magnetic characteristic of sediments from Gonghai Lake, Shanxi, North China. *Chin. Sci. Bull.* **2011**, *56*, 2464–2474.
14. Famera, M.; Babek, O.; Grygar, T.M.; Novakova, T. Distribution of heavy metal contamination in Regulated River-channel deposits: A magnetic susceptibility and grain-size approach; River Morava, Czech Republic. *Water Air Soil Pollut.* **2013**, *224*, 1525. [[CrossRef](#)]
15. Jordanova, D.; Hoffmann, V.; Fehr, K.T. Mineral magnetic characterization of anthropogenic magnetic phases in the Danube River sediments (Bulgarian part). *Earth Planet. Sci. Lett.* **2004**, *221*, 71–89. [[CrossRef](#)]
16. Xu, Y.; Sun, Q.; Yi, L.; Yin, X.; Wang, A.; Li, Y.; Chen, J. The source of natural and anthropogenic heavy metals in the sediments of the Minjiang Rivers Estuary (SE China): Implications for historical pollution. *Sci. Total Environ.* **2014**, *493*, 729–736. [[CrossRef](#)] [[PubMed](#)]
17. Aidona, E.; Grison, H.; Petrovsky, E.; Kazakis, N.; Papadopoulou, L. Magnetic characteristics and trace elements concentration in soils from Anthemountas River basin (North Greece): Discrimination of different sources of magnetic enhancement. *Environ. Earth Sci.* **2016**, *75*, 1375. [[CrossRef](#)]
18. Blaha, U.; Appel, E.; Stanjek, H. Determination of anthropogenic boundary depth in industrially polluted soil and semi-quantification of heavy metal loads using magnetic susceptibility. *Environ. Pollut.* **2008**, *156*, 278–289. [[CrossRef](#)] [[PubMed](#)]
19. Lu, S.G.; Bai, S.Q.; Xue, Q.F. Magnetic properties as indicators of heavy metals pollution in urban topsoils: A case study from the city of Luoyang, China. *Geophys. J. Int.* **2007**, *171*, 568–580. [[CrossRef](#)]
20. Zong, Y.; Xiao, Q.; Lu, S. Magnetic signature and source identification of heavy metal contamination in urban soils of steel industry city, Northeast China. *J. Soils Sediments* **2017**, *17*, 190–203. [[CrossRef](#)]
21. Bijaksana, S.; Huliselan, E.K. Magnetic properties and heavy metal content of sanitary leachate sludge in two landfill sites near Bandung, Indonesia. *Environ. Earth Sci.* **2010**, *60*, 409–419. [[CrossRef](#)]
22. Huliselan, E.K.; Bijaksana, S.; Srigutomo, W.; Kardena, E. Scanning electronic microscopy and magnetic characterization of iron oxides in solid waste landfill leachate. *J. Hazard. Mater.* **2010**, *179*, 701–708. [[CrossRef](#)] [[PubMed](#)]
23. Kirana, K.H.; Aufa, N.; Huliselan, E.K.; Bijaksana, S. Magnetic and Electrical Properties of Leachate. *ITB J. Sci.* **2011**, *43*, 165–178. [[CrossRef](#)]
24. Katili, J.A. Past and present geotectonic position of Sulawesi, Indonesia. *Tectonophysics* **1978**, *45*, 289–322. [[CrossRef](#)]
25. Bachri, S.; Sukido, S.; Ratman, N. *Geological Map of the Tilamuta Quadrangle, Sulawesi, 1:250,000*; Geological Research and Development Centre: Bandung, Indonesia, 2012.
26. Bachri, S.; Sidarto, S. Tektonik Sulawesi. In *Geologi Sulawesi*; Surono, S., Hartono, U., Eds.; LIPI Press: Bandung, Indonesia, 2013; pp. 303–324. ISBN 978-9797997571. (in Indonesian with English abstract).
27. Sudarningsih, S.; Bijaksana, S.; Ramdani, R.; Hafidz, A.; Pratama, A.; Widodo, W.; Iskandar, I.; Dahrin, D.; Fajar, S.J.; Santoso, N.A. Variation in the concentration of magnetic minerals and heavy metals in suspended sediments from Citarum River and tributaries, West Java, Indonesia. *Geosciences* **2017**, *7*, 66. [[CrossRef](#)]
28. Dearing, J.A. *Environmental Magnetic Susceptibility Using the Bartington MS2 System*; Chi Publishing: Kenilworth, UK, 1994; pp. 5–48. ISBN 0952340909.
29. Dearing, J.A.; Dann, R.J.L.; Hay, K.; Lees, J.A.; Loveland, P.J.; Maher, B.A.; O'Grady, K. Frequency-dependent susceptibility measurements of environmental materials. *Geophys. J. Int.* **1996**, *124*, 228–240. [[CrossRef](#)]

30. Hannigan, R.E.; Sholkovitz, E.R. The development of middle rare earth element enrichments in freshwaters: Weathering of phosphate minerals. *Chem. Geol.* **2001**, *175*, 495–508. [[CrossRef](#)]
31. Song, H.; Shin, W.J.; Ryu, J.S.; Shin, H.S. Anthropogenic rare earth elements and their spatial distributions in the Han River, South Korea. *Chemosphere* **2017**, *172*, 155–165. [[CrossRef](#)] [[PubMed](#)]
32. Tamuntuan, G.; Bijaksana, S.; Gaffar, E.; Russell, J.; Safiuddin, L.O.; Huliselan, E. The magnetic properties of Indonesia lake sediment: A case study of a Tectonic Lake in South Sulawesi and Maar Lakes in East Java. *ITB J. Sci.* **2010**, *42*, 31–48. [[CrossRef](#)]
33. Venkatachalapathy, R.; Rajeswari, V.; Basavaiah, N.; Balasubramanian, T. Environmental magnetic studies on surface sediments: A proxy for metal and hydrocarbon contamination. *Int. J. Environ. Sci. Technol.* **2014**, *11*, 2061–2074. [[CrossRef](#)]
34. Reyes, B.A.; Bautista, F.; Goguitchaichvili, A.; Conteres, J.J.M.; Owen, P.Q.; Carvallo, C.; Battu, J. Rock-magnetic properties of topsoils and urban dust from Morelia (>80,000 inhabitants), Mexico: Implication for anthropogenic pollution monitoring in Mexico's medium size cities. *Geofis. Int.* **2013**, *52*, 121–133.
35. Li, Y.X.; Yu, Z.; Kodama, K.P.; Moeller, R.E. A 14,000-year environmental change history revealed by mineral magnetic data from White Lake, New Jersey, USA. *Earth Planet. Sci. Lett.* **2006**, *246*, 27–40. [[CrossRef](#)]
36. Cao, L.; Appel, E.; Hu, S.; Yin, G.; Lin, H.; Rösler, W. Magnetic response to air pollution recorded by soil and dust-loaded leaves in a changing industrial environment. *Atmos. Environ.* **2015**, *119*, 304–313. [[CrossRef](#)]
37. Mariyanto, M.; Bijaksana, S. Magnetic properties of Surabaya River sediments, East Java, Indonesia. *AIP Conf. Proc.* **2017**, *1861*, 030045. [[CrossRef](#)]
38. Wang, X.S.; Qin, Y. Magnetic properties of urban top soils and correlation with heavy metals: A case study from the city of Xuzhou, China. *Environ. Geol.* **2006**, *49*, 897–904. [[CrossRef](#)]
39. Chakarvorty, M.; Dwivedi, A.K.; Shukla, A.D.; Kumar, S.; Niyoga, A.; Usmani, M.; Pati, J.K. Geochemistry and magnetic measurements of suspended sediment in urban sewage water vis-à-vis quantification of heavy metal pollution in Ganga and Yamuna Rivers, India. *Environ. Monit. Assess.* **2015**, *187*, 604. [[CrossRef](#)] [[PubMed](#)]
40. Attia, O.E.A.; Ab Khadra, A.M.; Nawwar, A.H.; Radwan, G. Impacts of human activities on the sedimentological and geochemical characteristics of Mabahiss Bay, North Hurghada, Red Sea, Egypt. *Arab. J. Geosci.* **2012**, *5*, 481–499. [[CrossRef](#)]
41. Naimi, S.; Ayoubi, S. Vertical and horizontal distribution of magnetic susceptibility and metal contents in an industrial district of central Iran. *J. Appl. Geophys.* **2013**, *96*, 55–66. [[CrossRef](#)]
42. Zhang, C.; Qiao, Q.; Appel, E.; Huang, B. Discriminating sources of anthropogenic heavy metals in urban street dusts using magnetic and chemical methods. *J. Geochem. Explor.* **2012**, *119–120*, 60–75. [[CrossRef](#)]
43. Hissler, C.; Hostache, R.; Iffly, J.F.; Pfister, L.; Stille, P. Anthropogenic rare earth element fluxes into floodplains: Coupling between geochemical monitoring and hydrodynamic sediment transport modeling. *C. R. Geosci.* **2015**, *327*, 294–303. [[CrossRef](#)]
44. Fernandes, L.L.; Kessarkar, P.M.; Parthiban, G.; Purnachandra Rao, V. Changes in depositional environment for the past 35 years in the Thane Creek, central west coast of India: Inferences from REEs, metals and magnetic properties. *Environ. Earth Sci.* **2017**, *76*, 189. [[CrossRef](#)]
45. Sklyarova, O.A.; Sklyarov, E.V.; Och, L.; Pastukhov, M.V.; Zagorulko, N.A. Rare earth elements in tributaries of Lake Baikal (Siberia, Russia). *Appl. Geochem.* **2017**, *82*, 164–176. [[CrossRef](#)]
46. Šmuc, N.R.; Serafimovski, T.; Dolenec, T.; Delenec, M.; Vrhovnik, P.; Vrabec, M.; Jačimović, R.; Zorn, V.L.; Komar, D. Mineralogical and geochemical study of Lake Dojran sediments (Republic of Macedonia). *J. Geochem. Explor.* **2015**, *150*, 73–83. [[CrossRef](#)]
47. Klaver, G.; Verheul, M.; Bakker, I.; Girauld, E.P.; Nègre, P. Anthropogenic rare earth elements in rivers: Gadolinium and Lanthanum partitioning between the dissolved and particulate phase in the Rhine River and spatial propagation through the Rynne—Meuse delta (The Netherlands). *Appl. Geochem.* **2014**, *47*, 186–197. [[CrossRef](#)]
48. Girauld, E.P.; Klaver, G.; Nègre, P. Natural versus anthropogenic sources in the surface-and groundwater dissolved load of the Dommel River (Meuse basin): Constraints by boron and strontium isotopes and gadolinium anomaly. *J. Hydrol.* **2009**, *369*, 336–349.

